

Effect of Bi alloying on the hole transport in the dilute bismide alloy GaAs_{1-x}Bi_x

R. N. Kini,* A. J. Ptak, B. Fluegel, R. France, R. C. Reedy, and A. Mascarenhas

National Renewable Energy Laboratory, 1617 Cole Boulevard, Golden, Colorado 80401, USA

(Received 12 August 2010; revised manuscript received 7 January 2011; published 16 February 2011)

We studied the effect of Bi incorporation on the hole mobility in the dilute bismide alloy GaAs_{1-x}Bi_x using electrical transport (Hall) and photoluminescence (PL) techniques. Our measurements show that the hole mobility decreases with increasing Bi concentration. Analysis of the temperature-dependent Hall transport data of *p*-type GaAsBi epilayers along with low-temperature PL measurements of *p*-doped and undoped epilayers suggests that Bi incorporation results in the formation of several trap levels above the valence band, which we attribute to Bi-Bi pair states. The decrease in hole mobility with increasing Bi concentration can be explained as being caused by scattering at the isolated Bi and the Bi-Bi pair states. We also observed a decrease in hole concentration with Bi incorporation. We believe that Bi_{Ga} heteroantisite defects compensate the acceptors, thus reducing the effective hole concentration.

DOI: [10.1103/PhysRevB.83.075307](https://doi.org/10.1103/PhysRevB.83.075307)

PACS number(s): 78.55.Cr, 72.20.Fr, 71.55.Eq

I. INTRODUCTION

The dilute bismide alloy GaAs_{1-x}Bi_x has attracted a lot of interest in recent years due to its unusual properties such as giant band-gap bowing^{1,2} and spin-orbit bowing,³ and its potential technological applications in high-efficiency solar cells,⁴ heterojunction bipolar transistors (HBTs),⁵ spintronics, and near-infrared devices. It is complementary to the well-studied dilute nitride alloy GaAs_{1-x}N_x because incorporating Bi in GaAs perturbs the valence band, whereas N in GaAs perturbs the conduction band. Both alloys show a giant band-gap bowing effect in which a small amount of Bi or N causes a large reduction in the band gap.^{1,2,6,7} Isolated N forms a resonant state in the conduction band of GaAs, and N pairs and clusters form bound states in the gap. N incorporation in GaAs causes a reduction in the electron mobility due to strong carrier scattering at localized states due to isolated N and N-cluster states.⁸ It has been theoretically shown that the isolated Bi impurity will form a resonant state in the valence band of GaAs.⁹ Even though experimental evidence for the isolated Bi state in GaAs has not been reported, there is experimental evidence for bound states due to pairs or clusters of Bi in GaAs.^{10,11} By comparing the case of GaAsN and GaAsBi, one might expect Bi alloying to affect the hole mobility in the case of GaAsBi.

There have been several optical and structural studies of the dilute bismide alloy, but few on electrical transport characteristics. Recently, using Hall transport measurements, we showed that Bi incorporation does not degrade the electron mobility.¹² In this paper we present a detailed study of the hole mobility in *p*-doped GaAsBi epilayers using Hall transport and photoluminescence (PL) measurements. Our measurements show that unlike electron mobility, the hole mobility decreases with increasing Bi concentration. Analysis of the Hall data reveals that Bi incorporation introduces deep trap levels above the valence band, which we attribute to Bi-Bi pair states. PL measurements on undoped epilayers also confirm the existence of these levels, consistent with the Hall data of *p*-doped epilayers. We suggest that the decrease in hole mobility with increasing Bi concentration is due to

hole scattering at the isolated Bi state and the Bi-Bi pair states.

II. EXPERIMENT

GaAsBi epilayers of thickness 0.3–0.5 μm were grown on semi-insulating, undoped GaAs substrates using molecular beam epitaxy (MBE) and the details about the growth can be found in Ref. 12. High-resolution x-ray diffraction (XRD) measurements of symmetric (004) reflections were used to estimate the concentration of Bi using the extrapolated GaBi lattice constant of 6.33 Å.¹³ XRD reciprocal space maps of asymmetric (224) reflections were performed on selected samples to ensure that all growths were pseudomorphic. The epilayers used for Hall measurements were doped with either C or Be. The doped epilayers were etched into a cloverleaf pattern and electroplated Au was used as ohmic contacts. The carrier density and mobility data were obtained using the van der Pauw technique on as-grown samples. The measurements were carried out in the low electric field regime, i.e., in the “ohmic” regime that was identified from *I*(*V*) conductivity measurements carried out from negative to positive bias, giving us a certainty about the linearity of the contact resistance in all the measured samples. For carrying out the Hall measurements, the samples were mounted on the cold finger of a closed cycle cryostat placed between the poles of an electromagnet. The Hall transport measurements were carried out at temperatures ranging from ~10 to 295 K. All connections between the cryostat and the Hall measurement system were made using triaxial cables and the measurements were performed in guarded mode to avoid parasitic capacitance. For the temperature- and power-dependent PL measurements a Nd-yttrium aluminum garnet (YAG) laser emitting at 532 nm was used as the excitation source. PL emission was dispersed by a Spex 270M spectrometer and detected using a cooled charge-coupled device (CCD). For time-resolved PL (TRPL) measurements, frequency-doubled pulses (~404 nm) from a Ti-sapphire amplifier (~150 fs) were used as the excitation source and PL was detected using an infrared photomultiplier tube (IRPMT).

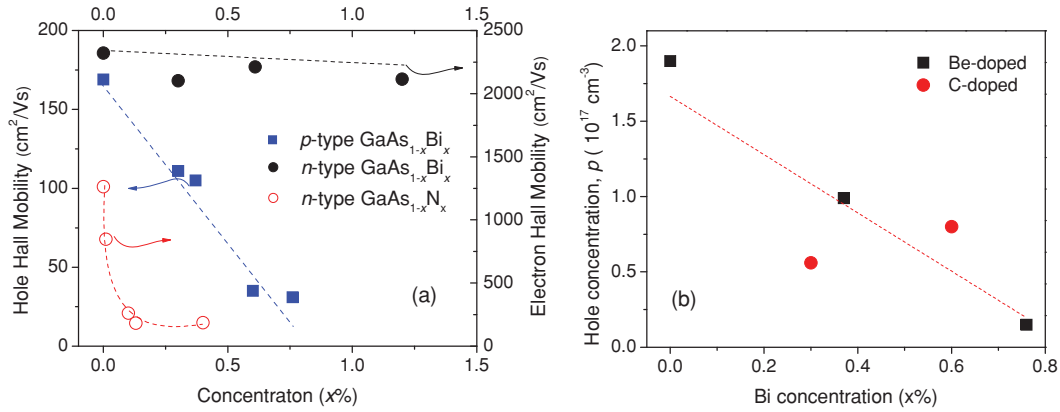


FIG. 1. (Color online) (a) RT hole Hall mobility of p -type $\text{GaAs}_{1-x}\text{Bi}_x$ epilayers. For comparison, electron Hall mobility data of n -type GaAsBi and GaAsN samples taken from Refs. 12 and 14, respectively, is also shown. (b) The hole concentration at RT for p -type $\text{GaAs}_{1-x}\text{Bi}_x$ epilayers. The dotted lines are a guide to the eye.

III. RESULTS AND DISCUSSION

A. p -type samples

We performed temperature-dependant Hall transport measurements and PL measurements on C- and Be-doped $\text{GaAs}_{1-x}\text{Bi}_x$ epilayers. Figure 1(a) shows the room-temperature (RT) hole Hall mobility of the samples. A decrease in the hole mobility with increasing x was observed for the p -type samples. For comparison, electron Hall mobility of n -type GaAsBi (Ref. 12) and GaAsN (Ref. 14) samples reported earlier is also shown in Fig. 1(a). Electron mobility did not show significant degradation with Bi alloying while a drastic (almost exponential) reduction in the electron mobility was observed with N incorporation in GaAs . As reported earlier, N incorporation in GaAs causes a reduction in the electron mobility owing to strong carrier scattering at the localized states due to isolated N and N-cluster states.⁸ Our observations show that Bi incorporation causes degradation of the hole mobility in GaAs . This can be understood by considering the fact that isolated Bi and pairs and/or clusters of Bi generate potential trap states for holes [schematically shown in Fig. 4(d)], which can lead to a decrease in hole mobility due to scattering at these states. A most recent report agrees well with our observation that Bi incorporation causes degradation of the hole mobility in GaAs .¹⁵

Figure 1(b) shows the variation of hole concentration at RT with Bi incorporation. A decrease in hole concentration with Bi incorporation was observed. The Be flux was maintained at the same level while growing the different samples, and secondary-ion-mass spectroscopy (SIMS) measurements indicate that Be concentration is similar in all of the samples ($\sim 2 \times 10^{17} \text{ cm}^{-3}$). This suggests that in the case of Be-doped samples, the hole concentration decreases with increasing Bi concentration. SIMS measurements on C-doped samples indicate a similar concentration of carbon in both the samples ($\sim 5 \times 10^{17} \text{ cm}^{-3}$). Comparing this with the observed hole concentration in Hall measurements ($0.6\text{--}0.8 \times 10^{17} \text{ cm}^{-3}$) of the C-doped samples, even though a monotonic decrease of the hole concentration with increasing Bi concentration cannot be unambiguously inferred, it is clear that Bi incorporation causes an overall decrease in the hole concentration. This suggests that

the dopants are either compensated¹⁶ or form complexes that passivate the dopants.¹⁷ Similar behavior has been reported for GaInNAs alloys, where the electron concentration was observed to decrease with increase in N concentration, and it was suggested that N-related localized states or complexes were compensating the donors.¹⁷ In the case of GaAsBi , it has been shown that a fraction (up to 10%) of the total Bi content occupies the Ga site and acts as singly ionized double donors.¹⁸ We believe that these Bi_{Ga} heteroantisite defects result in the compensation of the acceptors, thus reducing the effective hole concentration. However, further experiments are required to confirm the presence of Bi_{Ga} heteroantisite defects. Extended x-ray absorption fine-structure spectroscopy (EXAFS) was used to investigate the atomic neighborhood and local distortions around Bi atoms in GaAsBi .¹⁹ Such measurements may be useful to confirm the presence of Bi_{Ga} heteroantisite defects.

Figure 2 shows the variable temperature Hall data obtained for Be-doped samples. A similar temperature dependence of the mobility and carrier concentration was observed for the C-doped samples (not shown). The mobility of the sample with no bismuth doping ($x = 0$) shows a temperature dependence that is typical for p -type GaAs .²⁰ Due to the decrease in phonon scattering, the mobility increases as the temperature is decreased from 300 to 185 K. For $T < 185$ K ionized impurity scattering becomes the dominant mobility-limiting scattering mechanism and mobility decreases as the temperature is decreased. The sample with 0.37% Bi has a lower 300 K mobility compared to the sample with no bismuth. The temperature dependence of the mobility is similar to the sample with no bismuth—the mobility increases as the temperature is decreased up to 160 K, then decreases as the temperature is further decreased. The temperature dependence of the hole mobility can be analyzed assuming a typical temperature dependence for the various fundamental scattering mechanisms—for ionized impurity scattering, $\mu_{\text{II}} \sim T^{3/2}$, and for lattice scattering, $\mu_{\text{latt}} \sim T^{-3/2}$. If each scattering mechanism contributes simultaneously and independently, then the net mobility is given by the Matthiessen relation, $\mu = [\mu_{\text{II}} + 1/\mu_{\text{latt}}]^{-1}$. The temperature dependence of the mobility for the sample with $x = 0$ and 0.37% can be estimated using ionized impurity

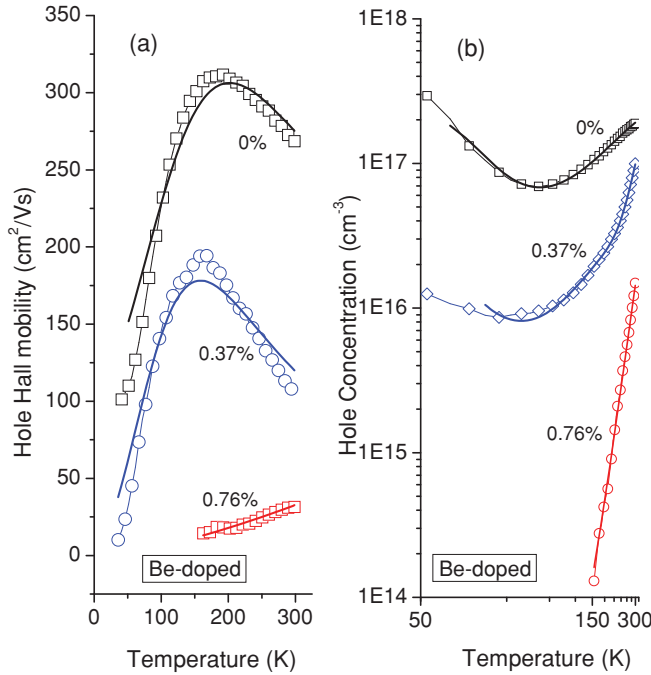


FIG. 2. (Color online) (a) The hole mobility and (b) the hole concentration of Be-doped $\text{GaAs}_{1-x}\text{Bi}_x$ samples as a function of temperature. The solid lines are fits to the data.

and lattice scattering as shown in Fig. 2(a). The temperature dependence of the hole mobility for the sample with 0.76% Bi is quite different from the sample with 0.37% Bi; the mobility decreases with decrease in temperature, which can be approximated by a $T^{3/2}$ dependence. This behavior can be explained using ionized impurity scattering limited mobility ($\mu_{II} \sim T^{3/2}$), which suggests that at higher Bi concentrations ionized impurity scattering is the dominant mobility limiting mechanism.

Figure 2(b) shows the variable temperature carrier-concentration data for Be-doped samples. For the sample with $x=0$, the hole concentration decreases as the temperature is lowered due to the freeze-out of holes onto acceptor sites. The hole concentration reaches a minimum of $\sim 7 \times 10^{16} \text{ cm}^{-3}$ at $\sim 92 \text{ K}$, and then appears to increase at lower temperatures, indicating impurity band conduction. At this doping concentration ($\sim 10^{17} \text{ cm}^{-3}$) the dopants are

close enough for their wave function to overlap and form an impurity band. This impurity band conduction is also evidenced in the variation of resistivity with temperature (not shown). Impurity band conduction is also seen in the sample with $x=0.37\%$. For the sample with $x=0.76\%$ the carrier concentration decreases as the temperature is decreased and it does not show any impurity band formation. If an impurity band is formed, the effective hole concentration can be calculated as²¹

$$p_h = \frac{(p_v + \gamma p_i)^2}{(p_v + \gamma^2 p_i)},$$

where p_v and p_i are the hole concentrations in the valence and impurity bands, respectively, and $\gamma = \frac{\mu_i}{\mu_v}$ is the ratio of the impurity and valence-band mobility. The hole concentration in the valence band p_v can be calculated using the neutrality equation given by²²

$$p_v + N_D = \sum_{i=1}^k \left[\frac{N_{A_i}}{1 + p/\phi_{A_i}} \right],$$

where $\phi_{A_i} = \frac{2(2\pi m_p^* k_B)^{3/2}}{h^3} g_{A_i} T^{3/2} e^{-E_{A_i}/k_B T}$ and N_{A_i} , E_{A_i} , and g_{A_i} are the concentration, activation energy, and degeneracy factor, respectively, for the i th acceptor. N_D is the total donor concentration, m_p^* is the hole effective mass, and h is Planck's constant. The hole concentration in the impurity band is equal to $p_i = \sum_{i=1}^k N_{A_i} - N_D - p_v$. The p -vs- T curve for the sample with $x=0$ was fitted using a single acceptor model with $E_{A_1} = 40 \text{ meV}$. The data for the sample with $x=0.3\%$ and 0.37% were fitted using a two-acceptor charge balance equation, and a single-acceptor model was sufficient for fitting the data for the samples with $x=0.6\%$ and 0.76% . Table I gives the values of the parameters used for fitting the experimental data. Because there are a large number of free parameters while attempting to fit the experimental data to the above equation, it is difficult to find unique values for the activation energy and hole concentration. However, the fitting exercise gives a good estimate for the parameter values and shows that Bi incorporation introduces a deep trap level, E_{A_2} , at $\sim 167\text{--}224 \text{ meV}$ above the valence band. The transport properties are mainly influenced by this level at higher Bi concentrations ($x \geq 0.6\%$). We believe that the E_{A_1} level may be due to the acceptors. Localized states due to

TABLE I. Characteristics of the $\text{GaAs}_{1-x}\text{Bi}_x$ samples studied: Parameters used for fitting the temperature-dependent transport data, the estimated concentration of Bi-Bi pairs and triplets, and the binding energy of the exciton corresponding to the PL peaks at $\sim 10 \text{ K}$.

Bi concentration ($x\%$)	Analysis of transport data ^a					Calculated concentration of		Binding energy corresponding to the PL peaks, E_b (meV)	
	E_{A_1} (meV)	E_{A_2} (meV)	$N_{A_1} \times 10^{16} \text{ cm}^{-3}$	$N_{A_2} \times 10^{18} \text{ cm}^{-3}$	γ	Pairs $\times 10^{18} \text{ cm}^{-3}$	Triplets $\times 10^{18} \text{ cm}^{-3}$		
0	40	–	27	–	0.078	–	–	28	
0.3	56	182	1.3	1.25	0.0007	3.3	0.18	81	178
0.37	55	167	3.3	2	0.001	4.9	0.33	80	160
0.6	–	213	–	11	–	12	1.3	–	157
0.76	–	224	–	0.55	–	18	2.5	–	139

^a $N_D = 0$ was used for all the samples except for the sample with $x=0$, for which $N_D = 1.5 \times 10^{16} \text{ cm}^{-3}$ gave a good fit to the experimental data.

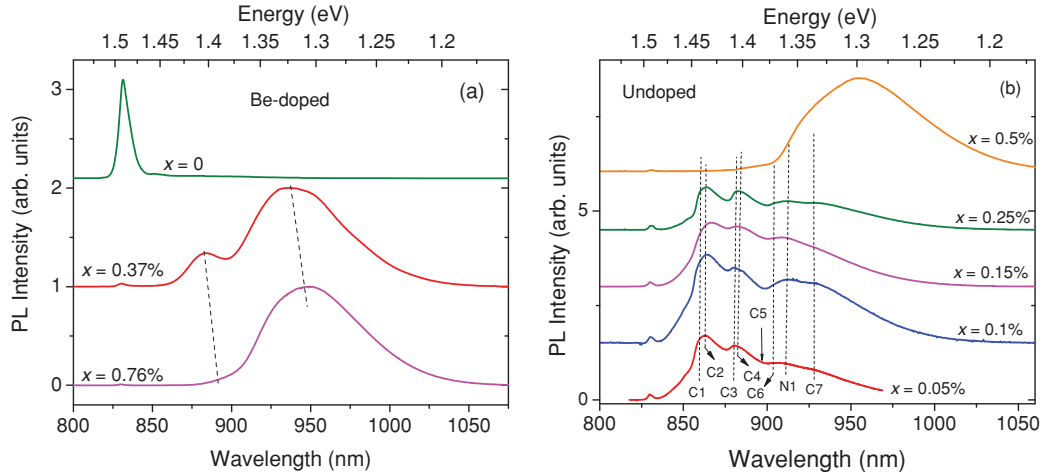


FIG. 3. (Color online) Low-temperature (~ 10 K) PL data for (a) Be-doped and (b) undoped $\text{GaAs}_{1-x}\text{Bi}_x$ samples.

Bi incorporation have been reported by others using optical studies of dilute bismides.^{10,23} To correlate the trap levels observed in our transport measurements with those observed in optical studies, we have done PL measurements which are described below.

Figure 3(a) shows low-temperature (~ 10 K) PL data for Be-doped $\text{GaAs}_{1-x}\text{Bi}_x$ samples. For the sample with $x = 0.37\%$ it is possible to resolve two peaks at ~ 1.40 and 1.32 eV. For the sample with $x = 0.76\%$ the emission is dominated by the lowest-energy peak at ~ 1.30 eV. The emission peaks show a redshift with increasing Bi concentration. If we assume that Bi causes a band-gap reduction of 90 meV per % of Bi [see inset of Fig. 4(a)], and use the free excitonic (FE) band gap of GaAs, $E_{\text{FE}}^{\text{GaAs}}$, we can calculate the binding energy corresponding to PL peaks $E_b = E_{\text{FE}}^{\text{GaAs}} - x \times 90 \text{ meV} - E_{\text{PL}}$. For the sample with $x = 0.37\%$ we obtained binding energies of ~ 80 and 160 meV and for the sample with 0.76% Bi, a binding energy of ~ 139 meV is obtained. Similar values were obtained for the C-doped samples. Hence PL data also suggest that Bi introduces a deep trap level (>100 meV) that qualitatively agrees with the transport data.

The concentration of the E_{A2} level obtained from fitting the carrier transport data is approximately two orders of magnitude smaller than the estimated concentration (0.6 – $1.5 \times 10^{20} \text{ cm}^{-3}$) of isolated Bi atoms assuming a random distribution of Bi atoms in the lattice. This suggests that these deeper levels could be due to pairs or clusters of Bi, which are expected to be present in lower concentrations. The concentration of the clusters of Bi can be estimated as the product of the total Bi atoms ($x \times 2.2 \times 10^{22} \text{ cm}^{-3}$) and the probability for each cluster.²⁴ The total concentration for different pair and triplet configurations is also given in Table I. The total concentration was calculated assuming nearest-neighbor (nn) and next-nearest-neighbor (nnn) interactions by following the method given in Ref. 24. There is reasonable agreement between the estimated pair concentration and the concentration of the E_{A2} level obtained from data fitting, except for the Be-doped sample with $x = 0.76\%$. This shows that the E_{A2} level may be due to Bi-Bi pairs. To further understand the nature of the trap levels due to Bi, we performed PL measurements on a series of undoped epilayers in which

the analysis of the data is slightly simplified since there are no acceptors. These measurements are described in the next section.

B. Undoped samples

Figure 3(b) shows low-temperature (~ 10 K) PL for the undoped samples with different Bi concentrations, $0.05\% \leq x \leq 1.4\%$. For samples with $x \leq 0.25\%$ several emission peaks labeled C1–C7 are seen and the spectrum is similar to that reported by Francoeur *et al.*¹⁰ In Ref. 10 it was proposed that C1 and C2 may be due to clusters of Bi and C3, C6, and C7 were assigned as the phonon replicas of C1 and C2. However, some of the peaks had to be excluded (C5 in Ref. 10, N1 in our case) while assigning the peaks as phonon replicas and there is only an approximate agreement between the peak energy separation and the LO phonon energy. We believe that these emission peaks may be due to Bi-Bi pairs with different lattice spacing, similar to the case of N-N pairs in GaPN,²⁵ with the lower-energy peaks corresponding to the pairs with the smallest pair separation. The following observations support this assignment.

(i) As the Bi concentration is increased the lower-energy peaks dominate the PL spectrum, because the probability of the closest pairs increases.

(ii) As shown in Fig. 4(a), when the temperature is increased, the intensity of the higher-energy peaks reduces compared to the lower-energy peaks. This is because as the temperature is increased the exciton, which is bound to the center with a small binding energy is thermally released. Also, for the centers with small binding energy there will be an opportunity for the exciton to tunnel to a lower-energy state (closer pairs) and decay there.²⁶ This latter process also explains why the higher-energy peaks are missing in the concentrated samples ($x > 0.25\%$), because in the concentrated samples the probability of closer pairs and hence the tunneling probability to lower-energy pairs is higher. As shown in Fig. 4(a), as the temperature is increased, the emission from the higher-energy peaks quench and eventually only a broad peak remains. The inset of Fig. 4(a) shows the energy of PL peaks as a function of the Bi concentration at 70 K for the

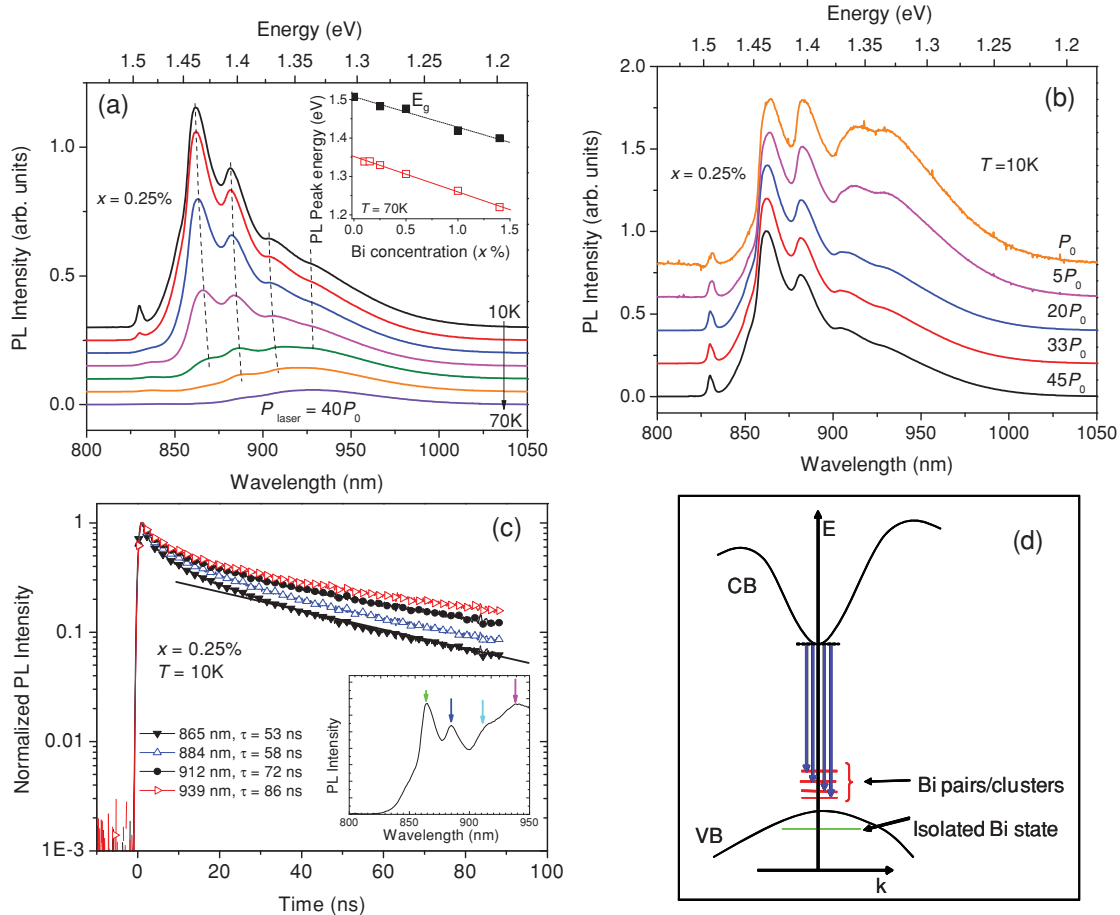


FIG. 4. (Color online) (a) PL at different temperatures for GaAs_{1-x}Bi_x sample with $x=0.25\%$ at a laser excitation power of 1.2 mW. The inset shows the PL peak energy as well as the band gap, E_g , at 70 K as a function of Bi concentration, x . E_g was obtained using modulated reflectance measurements. (b) PL curves for the sample with $x=0.25\%$ at 10 K for different excitation powers. P_0 refers to a laser excitation power of $30 \mu\text{W}$. (c) TRPL data for the sample with $x=0.25\%$ at 10 K obtained in a 10 nm window centered around 865, 884, 912, and 939 nm. The inset shows the PL obtained with 404 nm pulsed laser excitation. (d) A schematic representation of the isolated Bi and Bi-Bi pair states in GaAs.

samples with $0.1\% < x < 1.4\%$. From a linear fit to the data we obtain a redshift of 92 meV per% of Bi, which is close to the band-gap reduction due to Bi incorporation. This shows that the emission from the trap levels closely follows the band edge.

(iii) As shown in Fig. 4(b), when the excitation intensity is increased the emission shifts to high-energy peaks. This is because as the excitation intensity is increased the emission from the closest pairs saturate and recombination from the farthest pairs dominates.

These observations, the temperature and power dependence of the PL intensity of various peaks, cannot be explained by considering C3–C7 as phonon replicas of C1 and C2. Comparison of the PL spectra of undoped samples and the transport and/or PL measurements of p -doped samples discussed earlier, suggests that each of the emission peaks is owing to trap levels due to Bi-Bi pairs with different pair spacing. The temperature, power, and intensity dependence can be explained using exciton energy transfer between the various Bi-Bi levels. Similar concentration, temperature, and excitation power dependence was observed in the case of

N-N pairs in GaP and a stochastic model to explain this was developed by Leroux-Hugon *et al.*²⁷ Hence it is possible to conclude that Bi incorporation in GaAs results in the formation of several trap states above the valence-band edge as schematically shown in Fig. 4(d). These states act as scattering centers for holes and cause a reduction in the mobility.

We performed TRPL measurements to compare the lifetime (τ) and energy transfer processes in GaAsBi with GaPN.²⁸ Figure 4(c) shows the TRPL data obtained in a 10-nm window centered around 865, 884, 912, and 939 nm corresponding to C1 and C2, C3 and C4, N1, and C7 peaks, respectively. An exponential fit to the second half of the TRPL data was used to estimate the lifetime. Compared to the usual excitonic lifetime in GaAs (≤ 1 ns), these emission peaks show a long lifetime (~ 37 –86 ns). Similar to the case of N-N lines in GaPN,²⁸ as we move toward lower-energy states, τ increases. However, in contrast to N-N pairs in GaPN, the rise time is similar at all the emission peaks (Bi-Bi pair states) and is very short (~ 100 ps), which indicates very efficient energy transfer between the levels. To further understand the exciton dynamics at these Bi-Bi pair states, a detailed study of TRPL at different

temperatures and excitation powers is underway and will be reported later.

IV. CONCLUSIONS

We have studied the effect of Bi incorporation on the hole mobility in the dilute bismide alloy GaAs_{1-x}Bi_x using electrical transport (Hall) and PL techniques. Our measurements show that the hole mobility decreases with increasing Bi concentration. Analysis of the temperature-dependent Hall transport data of *p*-type GaAsBi epilayers along with low-temperature PL measurements of *p*-doped and undoped epilayers suggests that Bi incorporation results in the formation of several trap levels above the valence band. Comparison of the estimated Bi-Bi pair concentration and the concentration of the E_{A2} level obtained from fitting transport data suggest the trap levels to be due to Bi-Bi pair states. The decrease in hole mobility with increasing Bi concentration can be

understood as being caused by scattering at the isolated Bi and the Bi-Bi pair states. At higher Bi concentration ($x \geq 0.6\%$), the transport properties are mainly influenced by the E_{A2} level and the temperature dependence of the hole mobility can be approximated by a $T^{3/2}$ dependence. This suggests that at higher Bi concentration ionized impurity scattering is the dominant mobility limiting mechanism. We also observed a decrease in hole concentration with Bi incorporation. We believe that Bi_{Ga} heteroantisite defects compensate the acceptors, thus reducing the effective hole concentration.

ACKNOWLEDGMENTS

The authors would like to thank Michelle Young for processing the samples. This work was supported by the Department of Energy Office of Science, Basic Energy Sciences under Contract No. DE-AC36-08GO28308 with the National Renewable Energy Laboratory.

*Present address: Indian Institute of Science Education and Research, Thiruvananthapuram, Kerala, India; rajeevkini@iisertvm.ac.in

¹S. Francoeur, M.-J. Seong, A. Mascarenhas, S. Tixier, M. Adamcyk, and T. Tiedje, *Appl. Phys. Lett.* **82**, 3874 (2003).

²J. Yoshida, T. Kita, O. Wada, and K. Oe, *Jpn. J Appl. Phys., Part 1* **42**, 371 (2003).

³B. Fluegel, S. Francoeur, A. Mascarenhas, S. Tixier, E. C. Young, and T. Tiedje, *Phys. Rev. Lett.* **97**, 067205 (2006).

⁴F. Dimroth, *Phys. Status Solidi C* **3**, 373 (2006).

⁵P. M. Asbeck, R. J. Welty, C. W. Tu, H. P. Xin, and R. E. Welser, *Semicond. Sci. Technol.* **17**, 898 (2002).

⁶M. Weyers, M. Sato, and H. Ando, *Jpn. J. Appl. Phys., Part 2* **31**, L853 (1992).

⁷A. Mascarenhas, R. Kini, Y. Zhang, R. France, and A. Ptak, *Phys. Status Solidi B* **246**, 504 (2009).

⁸S. Fahy, A. Lindsay, H. Ouerdane, and E. P. O'Reilly, *Phys. Rev. B* **74**, 035203 (2006).

⁹Y. Zhang, A. Mascarenhas, and L.-W. Wang, *Phys. Rev. B* **71**, 155201 (2005).

¹⁰S. Francoeur, S. Tixier, E. Young, T. Tiedje, and A. Mascarenhas, *Phys. Rev. B* **77**, 085209 (2008).

¹¹Sebastian Imhof *et al.*, *Appl. Phys. Lett.* **96**, 131115 (2010).

¹²R. N. Kini, L. Bhusal, A. J. Ptak, R. France, and A. Mascarenhas, *J. Appl. Phys.* **106**, 043705 (2009).

¹³S. Tixier, M. Adamcyk, T. Tiedje, S. Francoeur, A. Mascarenhas, P. Wei, and F. Schiettekatte, *Appl. Phys. Lett.* **82**, 2245 (2003).

¹⁴D. L. Young, J. F. Geisz, and T. J. Coutts, *Appl. Phys. Lett.* **82**, 1236 (2003).

¹⁵D. A. Beaton, R. B. Lewis, M. Masnadi-Shirazi, and T. Tiedje, *J. Appl. Phys.* **108**, 083708 (2010).

¹⁶H. P. Xin, C. W. Tu, and M. Geva, *J. Vac. Sci. Technol. B* **18**, 1476 (2000).

¹⁷W. Li, M. Pessa, J. Toivonen, and H. Lipsanen, *Phys. Rev. B* **64**, 113308 (2001).

¹⁸M. Kunzer, W. Jost, U. Kaufmann, H. M. Hobgood, and R. N. Thomas, *Phys. Rev. B* **48**, 4437 (1993).

¹⁹G. Ciatto, E. C. Young, F. Glas, J. Chen, R. A. Mori, and T. Tiedje, *Phys. Rev. B* **78**, 035325 (2008).

²⁰S. A. Stockman, G. E. Höfler, J. N. Baillargeon, K. C. Hsieh, K. Y. Cheng, and G. E. Stillman, *J. Appl. Phys.* **72**, 981 (1992).

²¹H. Neumann, *Cryst. Res. Technol.* **23**, 1377 (1988).

²²*Semiconductor Statistics*, edited by J. S. Blakemore (Pergamon, New York, 1960).

²³G. Pettinari, A. Polimeni, M. Capizzi, J. H. Blokland, P. C. M. Christianen, J. C. Maan, E. C. Young, and T. Tiedje, *Appl. Phys. Lett.* **92**, 262105 (2008); R. Kudrawiec *et al.*, *J. Appl. Phys.* **106**, 023518 (2009).

²⁴M. M. Kreitman and D. L. Barnett, *J. Chem. Phys.* **43**, 364 (1965).

²⁵D. G. Thomas, J. J. Hopfield, and C. J. Frosch, *Phys. Rev. Lett.* **15**, 857 (1965); D. G. Thomas and J. J. Hopfield, *Phys. Rev.* **150**, 680 (1966).

²⁶P. J. Wiesner, R. A. Street, and H. D. Wolf, *Phys. Rev. Lett.* **35**, 1366 (1975).

²⁷P. Leroux-Hugon and H. Mariette, *Phys. Rev. B* **30**, 1622 (1984).

²⁸H. Mariette, *Physica B & C* **146B**, 286 (1987).